Available online at www.sciencedirect.com

SciVerse ScienceDirect

Ceramics International 38 (2012) 5157–5164

CERAMICS INTERNATIONAL

www.elsevier.com/locate/ceramint

How effective is the addition of nanoscaled particles to alumina–magnesia refractory castables?

E.Y. Sako *, M.A.L. Braulio, V.C. Pandolfelli

Federal University of São Carlos, Microstructural Materials Engineering Group (FIRE Associate Laboratory), Rod. Washigton Luiz, km 235, São Carlos, SP, Brazil

Received 7 February 2012; accepted 6 March 2012
Available online 15 March 2012

Abstract

The addition of nanoscaled alumina and magnesia particles to the matrix of alumina–magnesia refractory castables drastically reduces the residual expansion related to the *in situ* spinel formation. Nonetheless, as their benefits on other relevant properties have not been reported so far, the effectiveness of such nanoengineering design for castables applied in steel ladles is still uncertain. In the present work, not only the expansion level, but also the corrosion resistance, the hot modulus of rupture and the creep deformation of different nanoparticle-containing castables were evaluated and compared with the results attained by refractory materials designed only by micrometric-scaled Al_2O_3 and MgO. Although the addition of a nanoalumina and nanomagnesia mixture ensured the best results regarding to the expansive behavior, thermo-mechanical and thermo-chemical properties, its performance was only slightly superior to the castable containing micrometric alumina and magnesia particles. Therefore, as the cost–benefit ratio is one of the main requirements for the end users, the nanotechnology use in the refractory production must be previously carefully analyzed.

Keywords: D. Spinel; Nanotechnology; Refractory castables; Expansion

1. Introduction

According to Wagner's mechanism [1,2], due to the counter-diffusion of Mg^{2+} and Al^{3+} ions, magnesium aluminate spinel ($MgAl_2O_4$) formation takes place at both magnesia and alumina sides. At the magnesia particle, the reaction leads to a local shrinkage, whereas it is followed by expansion at the alumina interface. Therefore, the overall result depends on how much spinel is formed in each reactant side, which is defined by the spinel ratio thickness (R). Based on Wagner's results, Nakagawa [3] later found out that the R parameter can significantly change due to various factors. Among all of them, the sort and number of contacts between alumina and magnesia particles is the most important aspect for alumina–magnesia refractory castables.

In the matrix of such ceramic powder compacts, the following possibilities for the particle contacts can be found: MgO–MgO, MgO–Al_2O_3 and Al_2O_3–Al_2O_3. As stated by Nakagawa, the MgO–MgO contact does not add to the spinel expansion, as MgO shrinks after the reaction. On the other hand, MgO–Al_2O_3 and Al_2O_3–Al_2O_3 present a positive share on the castable volume change and the latter is the one with the higher increment. Thus, the R factor and, consequently the ΔV value, scale with the number of MgO–Al_2O_3 and Al_2O_3–Al_2O_3 pairs in the matrix.

In this context, changing the reactants' average grain size arises as an interesting tool to modify the amount of alumina and magnesia particles in the matrix, leading to a reduction in the number of the above-mentioned contact pairs and eventually in the overall expansion. In fact, Sako et al. [4] showed a significant decrease in the A/M ratio (number of alumina particles for each magnesia one in the composition) when replacing coarser MgO grains ($D < 100$ μm) by finer ones ($D < 13$ μm), which resulted in lower overall expansion values.

* Corresponding author at: Federal University of São Carlos, Materials Engineering Department, Microstructural Materials Engineering Group, FIRE Associate Laboratory, Rod. Washington Luiz, km 235, 13656-905 São Carlos, SP, Brazil.

E-mail addresses: eric.ysako@gmail.com (E.Y. Sako), vicpando@ufscar.br (V.C. Pandolfelli).

0272-8842/$36.00
doi:10.1016/j.ceramint.2012.03.021

Based on these fundamentals, Braulio et al. [5–7] evaluated the addition of nanoscaled particles in order to design and control the expansive behavior of spinel-forming castables. Novel advances in the use of nanotechnology in refractory compositions were reported in this study, mainly by adding a nanoengineered mixture of alumina and magnesia powders [7]. Based on this latter study, not only a volume change control was attained, but also the spinel reaction initiation could be speeded up as a consequence of the higher matrix reactivity.

However, despite the interesting benefits associated with the expansion control, the impact of adding such nanoscaled particles to other relevant properties, such as the corrosion resistance, the hot modulus of rupture and the creep deformation has not been reported so far. Considering these aspects, the main purpose of the present work was to evaluate the overall effectiveness of designing a nanoengineered matrix by comparing its benefits with those attained by castables containing micrometric-scaled particles in the matrix.

2. Materials and techniques

As conducted by Braulio et al. [7], the evaluation of adding different magnesia and alumina grain sizes to spinel-forming refractory castables was carried out based on a reference composition designed using tabular alumina as coarse aggregates (6 mm $\geq D \geq$ 0.2 mm, T-60, Almatis, Germany), 6 wt% of calcium aluminate cement as the binder (Secar 71, Kerneos, USA) and 1 wt% of microsilica (971 U, Elkem, Norway).

Firstly, only micrometric raw material sources were analyzed in the castable matrix (Table 1), due to the easier access and lower cost. MgO with three granulometric ranges ($D \leq 13$, $\leq$45 and $\leq$100 μm) were selected from the same dead-burnt magnesia source (95 wt% MgO, C/S = 0.37, Magnesita Refratários S.A., Brazil) and two alumina powder mixtures were tested: A1, fine tabular alumina ($D \leq 200$ μm) + reactive alumina CL 370 ($D \leq 10$ μm) and A2, in which portions of these two alumina sources were replaced by finer ones (tabular alumina ≤ 20 μm + reactive alumina A100 ($D \leq 4$ μm)).

Afterwards, a further reduction in the reactantś grain sizes was performed by adding nanoscaled particles. As a nanoalumina source, a colloidal alumina (CA) suspension with 50 wt% of solids concentration (VP Disp 650 ZXP, Evonik Degussa GmbH, Germany) was used. This aqueous dispersion is comprised by stabilized crystallites of 14 nm in size, with anionic characteristics and specific surface area of 100 m^2/g [8]. The same nanomagnesia powder presented by Braulio et al. [5] was selected for this work. This powder was prepared by centrifugal-type high energy ball milling, using a dead-burnt MgO ($D \leq 45$ μm, 95 wt% MgO, C/S = 0.37) as the starting material (steel ball grinding media/MgO ratio = 20:1). Fig. 1 shows the TEM (transmission electron microscopy) bright- and dark-field images for the magnesia particles after a milling time of 2 h [5]. The nanomagnesia particles, measured by the dark-field images, were mostly in the 10–20 nm range.

Moreover, a nanoscaled alumina–magnesia (AM) powder was prepared according to the procedure described for the nano MgO particles and also added to the matrix of the reference refractory composition. The initial materials used to produce this nanopowder were the reactive alumina CL370 and MgO $\leq$45 μm, resulting in, after high energy milling for 2 h, particles with crystallite sizes between 30 and 60 nm, as pointed out by transmission electron microscopy analysis (Fig. 2) [7].

The nanoscaled powder-containing castables were designed according to the procedure described by Braulio et al. [7], leading to the formulations presented in Table 2. In order to keep suitable castable particle packing (based on the Alfred packing model with $q = 0.26$), the addition of nanopowders was restricted to certain amounts. Higher increments would result in poor workability and spoil further evaluations. However, even though such a low content of colloidal alumina was used, some processing problems were faced. Due to gelling, large and isolated pores appeared in the castable's microstructure after curing, inhibiting some properties to be evaluated.

After processing the castables according to the procedure described by Sako et al. [9], cylindrical samples (50 mm × 50 mm, and central inner hole-diameter of 12.5 mm) of the compositions presented in Table 1 were shaped and their expansive behavior was evaluated by the assisted sintering technique in refractoriness-under-load equipment (Model RUL 421E; Netzsch, Germany). In this experiment, the sample's linear change is measured while it

Table 1
Matrix compositions of the evaluated castables containing micrometric particles. All of them comprised 62 wt% of coarse tabular alumina aggregates (6 mm ≥ D ≥ 0.2 mm), 6 wt% of CAC and 1 wt% of microsilica.

	Content (wt%)					
	M13 A1	M45 A1 (REF)	M100 A1	M13 A2	M45 A2	M100 A2
Dead-burnt MgO						
<3 μm	6	–	–	6	–	–
<45 μm	–	6	–	–	6	–
<100 μm	–	–	6	–	–	6
Tab. alumina < 200 μm	18	18	18	14	14	14
Tab. alumina < 20 μm	–	–	–	4	4	4
Reactive alumina CL370	7	7	7	3	3	3
Reactive alumina A1000	–	–	–	4	4	4

Table 2
Matrix compositions of the evaluated castables containing nano particles. All of them comprised 62 wt% of coarse tabular alumina aggregates (d < 6 mm), 6 wt% of CAC and 1 wt% of microsilica.

	Content (wt%)		
	Nano-MgO	CA	Nano-AM
Dead-burnt MgO < 45 μm	–	6	4
Nano-MgO	6	–	–
Nano-AM	–	–	7
Tabular alumina < 200 μm	18	18	15.3
Reactive alumina CL370	7	3	4.7
Colloidal alumina	–	4[a]	–

[a] 8 wt% of VP Disp 650 (colloidal alumina suspension with 50% of solids concentration) was used, which resulted in 4 wt% of solids in the castable composition.

is heated up to 1500 °C (3 °C/min) and maintained at this temperature for 5 h. After testing, the overall expansion value was attained and the castable apparent porosity was measured using the Archimedes technique in kerosene.

Hot modulus of rupture (HMOR) measurements were carried out under three-point bending tests (ASTMC 583) at 1450 °C using Netzsch 414/3 HMOR Equipment (Netzsch, Selb, Germany). For this test, prismatic samples (150 mm × 25 mm × 25 mm) were shaped and pre-fired at 1500 °C for 5 h, cooled at room temperature and then reheated for testing.

For the corrosion evaluation, samples were prepared in a 50 mm × 50 mm cylindrical shape with a 20 mm diameter × 25 mm depth internal hole, as reported by Sako et al. [10]. After pre-firing the samples at 1500 °C for 5 h, their internal holes were filled in with 10 g of a high-iron oxide steel ladle slag (Table 3) in order to perform the tests. The sample + slag set was then heated up to 1500 °C and the corrosion experiment was conducted for 2 h in air. The wear and penetration rates were calculated in order to measure the corrosion damage using the Image J 1.42q software (Wayne Rasband, National Institutes of Health, USA), according to the procedure described by Braulio et al. [11].

Table 3
Chemical composition of the industrial steel ladle slag used in this work.

Composition	MgO	Al_2O_3	SiO_2	CaO	MnO	Fe_2O_3
wt%	4.9	1.7	7.5	34.2	3.6	43.6

The creep tests were also conducted in the same refractoriness-under-load equipment used for the assisted sintering tests. For this evaluation, samples were pre-fired at 1550 °C for 24 h in order to inhibit sintering deformation during the experiment and, then heated up to 1450 °C (5 °C/min) and kept at this temperature for 24 h under a compression load of 0.2 MPa.

Scanning electron microscopy (SEM) images of the castables microstructure after firing at 1500 °C were attained (JEOL JSM-5900 lV, the Netherlands). Based on these images, the volume of pores and the pore size distribution in the castable matrix was estimated using image analyzer software (Image J 1.42q, Wayne Rasband, National Institutes of Health, USA).

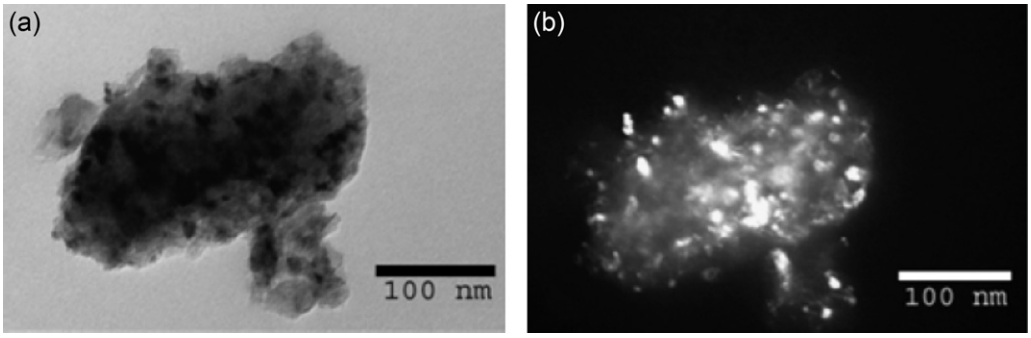

Fig. 1. TEM (a) bright-field and (b) dark-field images for the magnesia particles after high-energy milling time of 2 h [5].

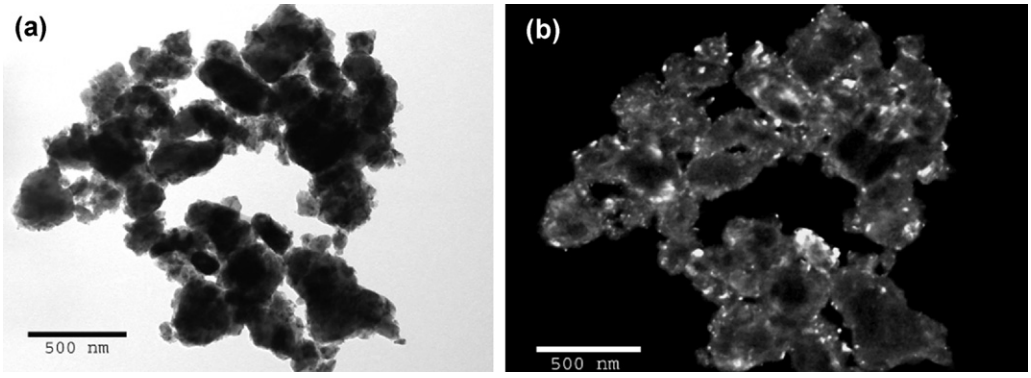

Fig. 2. TEM (a) bright-field and (b) dark-field images for the nanoscaled AM powder after high-energy milling time of 2 h [7].

Table 4
Overall expansion, initial spinel expansion temperature and apparent porosity after sintering at 1500 °C for 5 h of the alumina–magnesia castables containing different alumina and magnesia grain sizes.

	Overall expansion (%)		Initial spinel expansion temperature (°C)		Apparent porosity (%)	
	A1	A2	A1	A2	A1	A2
M13	2.2	1.9	1050	1105	20.4 ± 0.7	18.5 ± 0.9
M45	3.6	2.9	1065	1130	22.9 ± 0.4	20.4 ± 0.3
M100	5.3	4.5	1210	1370	31.3 ± 1.1	28.6 ± 0.7

Additionally, phase and microstructure evaluation of samples fired at 1150 °C or 1300 °C for 5 h were conducted by XRD quantitative analysis (TOPAS 4.1, Bruker, Karlsruhe, Germany).

3. Results and discussion

3.1. Reduction of alumina and magnesia grain size in the micrometric scale

Table 4 presents the overall expansion values of the alumina–magnesia castables containing micrometric-sized alumina and magnesia particles after the assisted sintering test (1500 °C for 5 h). A significant difference in the material's expansive behavior could be noticed by changing the reactants' grain size: adding finer magnesia particles resulted in lower expansion due to the spinel formation. As observed by Sako et al. [4], this result was induced by the lower number of Al_2O_3–Al_2O_3 pairs in the castable matrix, which usually counts as the largest portion of the volumetric changes. In addition, these authors also stated that the presence of finer magnesia grains helps to attain a higher sintering efficiency, decreasing the overall expansion value even more.

Still regarding Table 4, it is noticeable that, besides the effects of the magnesia particles, the reduction in the alumina grain size also played an important role in the castables' expansive behavior. For all evaluated magnesia sources (<100, <45 or <13 μm), adding finer alumina portions (A2) led to a lower residual expansion, which considering the mechanism described above, was not expected. Similar to the coarse magnesia composition (<100 μm), the incorporation of such alumina mixture also helps for a higher number of Al_2O_3–Al_2O_3 contact pairs in the castable matrix and, as a consequence, an increase in the linear change should have been detected. Nonetheless, as already stated by Braulio et al. [6], the more efficient sintering of fine alumina particles counterbalanced the spinel expansion, thus playing a more significant role on the castable overall expansion. This behavior was even more evident for the M100 castable, in which the Mg^{2+} diffusion rate is slower, resulting in a longer time for the alumina particles sintering. The delayed initial spinel expansion temperatures detected for the compositions containing finer alumina (A2) in Table 4 was a clear consequence of the higher alumina sintering effect.

These results pointed out that the correct selection of the raw materials grain size is a key issue for the spinel expansion control. Considering all the evaluated magnesia and alumina sources, it was possible to reduce the overall expansion from 5.3% to 1.9% only by changing this parameter. Such a variation induced direct consequences to the material's microstructural features. Castables with controlled expansive behavior presented, for example, more densified structures with lower apparent porosity after firing at 1500 °C for 5 h (Table 4). The combined use of MgO < 13 μm and alumina mixture A2 enabled reducing approximately 40% of the apparent porosity value when compared to those attained with the composition containing coarse grains (M100 A1).

Other relevant properties for spinel refractory castables applied to steel ladles could also be improved by this approach. A clear example is presented in Fig. 3 that shows the hot modulus of rupture (HMOR) values at 1450 °C for all evaluated castables pre-fired at 1500 °C for 5 h (which is the closest lab temperature condition to the working one). As can be observed in Table 1, all compositions comprised microsilica in the matrix and calcium aluminate cement as the binder, which leads to liquid formation in the quaternary system Al_2O_3–CaO–MgO–SiO_2 at reasonably high temperatures and spoils the material's hot properties [12,13]. However, the porosity decrease (Table 4) due to the fine magnesia and alumina particles (M13 A2) resulted in a suitable HMOR value. Comparatively, the attained mechanical strength for this composition was sixfold higher than the castable with M100 and A1, highlighting an important benefit of a designed microstructure to the refractory working life, which was attained just by changing the grain size.

Similarly, the corrosion resistance of the evaluated castables was affected by the alumina and magnesia grain sizes, as shown in Fig. 4. As reported by Sako et al. [12] and Braulio et al. [11], when in contact with high-FeO_x steel ladle slag, CAC-bonded *in situ* spinel forming castables usually present excellent corrosion resistance due to suitable microstructural features, in which CA_6 distribution helps to protect the refractory from the

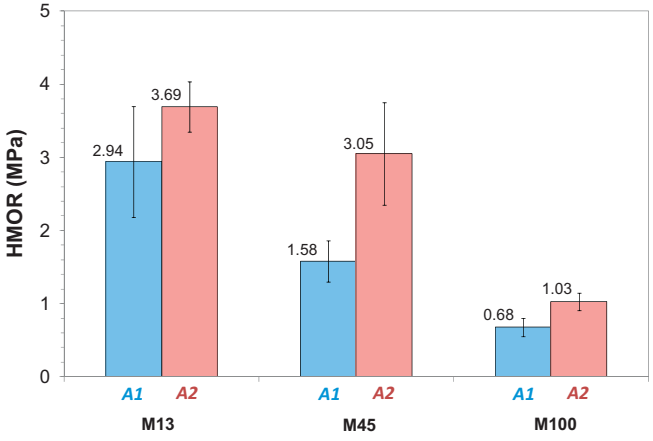

Fig. 3. Hot modulus of rupture (HMOR) at 1450 °C of the alumina–magnesia castables containing different alumina and magnesia grain sizes after pre-firing at 1500 °C for 5 h.

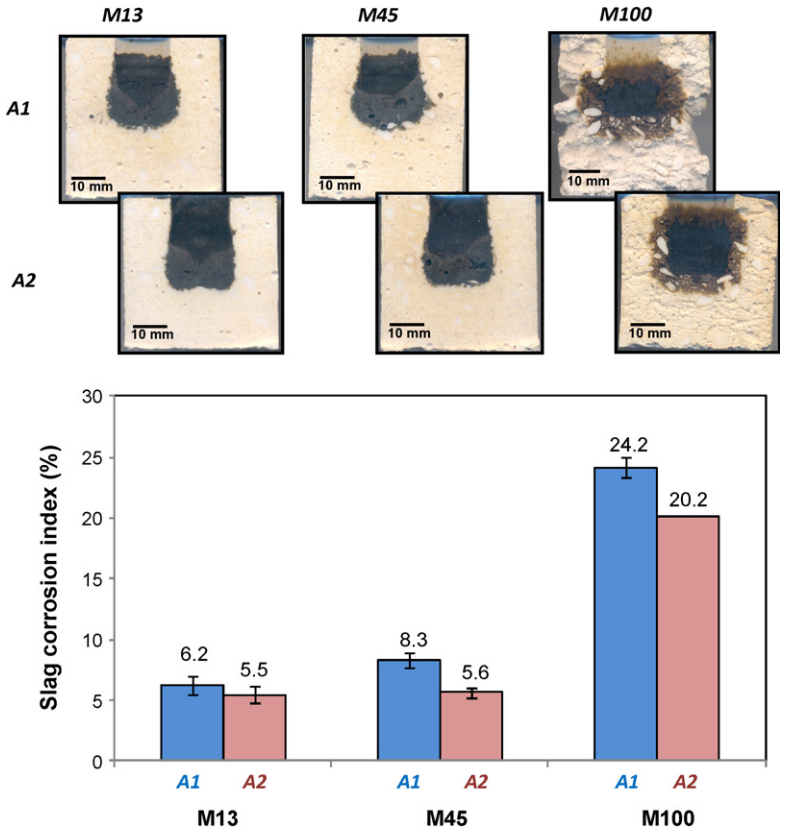

Fig. 4. Samples' cross-section and slag corrosion indexes of the alumina–magnesia castables containing different alumina and magnesia grain sizes after the corrosion experiments.

chemical attack. In these studies, the conclusions were drawn based on the composition M45 A1. Therefore, reducing the alumina and magnesia grain size would decrease the corrosion degree even more (as can be seen in Fig. 4), as a direct consequence of a lower open porosity. On the other hand, even presenting the same chemical and phase composition after firing at 1500 °C/5 h, the higher porosity of the castables containing coarse grains (mainly MgO) favored the slag physical infiltration.

These results showed that, depending on the reactants' grain size, the intrinsic benefits of the *in situ* spinel to the castable corrosion resistance can be spoiled by the Kirkendall effect, which is the mechanism responsible for the pore formation during the $MgAl_2O_4$ reaction [4,14,15]. Thus, the lower porosity and pore size values attained by the fine particles addition inhibited such a problem and ensured the well-known spinel corrosion resistance. Considering the HMOR and corrosion resistance improvements observed so far, the use of fine micrometric alumina and magnesia grains in the castable matrix seemed to be a suitable alternative to produce high-performance *in situ* spinel-forming refractories. Nevertheless, it also raises another question: would the results be even better with nanometric-sized particles addition?

3.2. Castable matrixes engineered by nanoscaled particles addition

Regarding only the expansive behavior, Braulio et al. [7] attempted to solve the above question by reporting the results presented in Fig. 5. In this graph, the effect of the addition of each nanoparticle source (CA, nano MgO and nano AM) on the castable overall expansion after the assisted sintering test (1500 °C for 5 h) and on its initial spinel expansion temperature is observed, comparatively to the results attained with micrometric particles (also presented in Table 4).

Due to its particularly higher reactivity, the use of nano MgO helped to reduce the initial spinel expansion temperature even more when compared to the previously micrometric evaluated sources. However, regarding the overall expansion, the attained value was close to the M13 one. As shown in a previous publication [5], part of these MgO nanopowders tend to

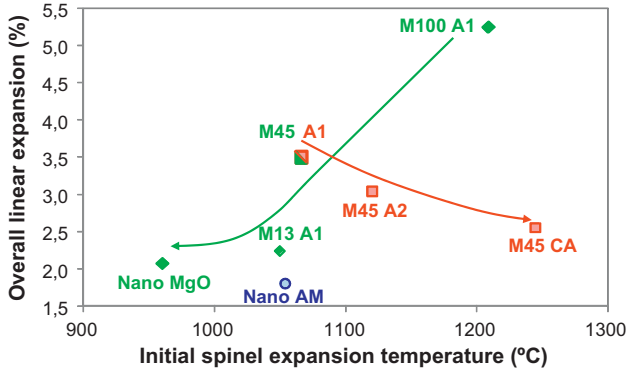

Fig. 5. Overall linear expansion after sintering at 1500 °C for 5 h as a function of the initial spinel expansion temperature of spinel castables containing different alumina and magnesia grain sizes [7].

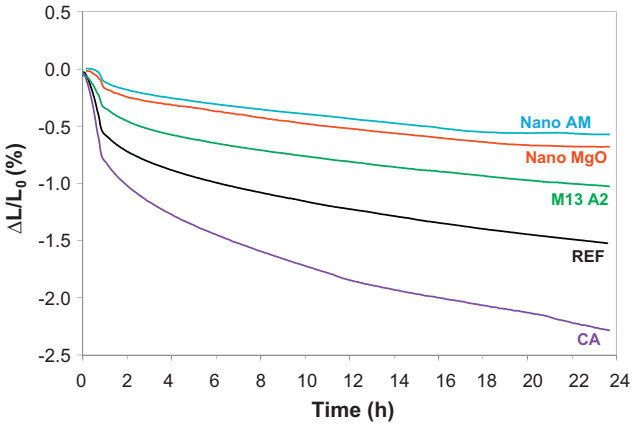

Fig. 6. Creep resistance at 1450 °C of the alumina–magnesia castables containing nano powders after firing for 24 h at 1550 °C. The results for REF (M45 A1) and M13 A2 castables are also plotted for comparison.

agglomerate and act like coarser aggregates during the spinel formation reaction, leading to this result.

Adding colloidal alumina led to a significant overall expansion reduction. Incorporated as an aqueous suspension (Table 2), these particles dispersed efficiently throughout the castable matrix, inhibiting agglomeration problems. Nonetheless, the nanoalumina presence delayed the initial spinel expansion temperature. As discussed in the previous topic, this result is associated with the higher alumina sintering degree, which counterbalances the spinel expansion. Hence, the more efficient the alumina particle sintering is, the higher the detected initial spinel expansion temperature is.

As an additional alternative, the use of a nanoscaled mixture of alumina and magnesia (nano AM) was also analyzed and seemed to be even more efficient to reduce the castable overall expansion. However, due to the enhanced delaying effects of the nanoalumina presence, the initial spinel expansion temperature was higher when compared to the nano MgO composition or even the M13 one. In order to evaluate the material's performance at working temperatures, Fig. 6 presents the creep deformation resistance of the alumina–magnesia castables containing nanoparticles. The results of the reference composition (REF-M45 A1) and of the best one containing micrometric particles (M13 A2) are also presented for comparison.

In order to understand the castable's creep deformation, three main aspects should be taken into consideration: the liquid content in the microstructure, the particle size and morphology, and the castable's porosity [16]. In other words, a good performance is achieved with the presence of a low amount of liquid, large grains and a densified structure. The material's chemical composition was kept constant and, then the liquid content after firing was basically the same for all evaluated compositions, based on previous thermodynamic simulation [13]. Therefore, the creep results in Fig. 6 were associated with the different microstructural development of each sample.

The nano MgO and nano AM addition clearly increased the castable creep resistance, leading to an excellent performance of the nano-engineered castables. This result was not expected, as the addition of such powders should generate finer spinel grains, as reported by Braulio et al. [7], and consequently, would reduce the creep resistance. Nonetheless, due to the presence of very reactivity MgO nano-particles, spinel formation was speeded up in both compositions, as pointed out in the quantitative XRD results in Table 5.

A greater amount of $MgAl_2O_4$ was already formed at 1150 °C in the nano MgO and nano AM compositions when compared to the ones containing micrometric particles. As stated in a previous work [4], this faster spinel reaction presents a direct consequence on the sintering efficiency afterwards. Therefore, after the pre-firing step for the creep experiments, the samples containing nanopowders presented a much more densified structure, with a reduced volume of pores (Fig. 7a) and pore size distribution (Fig. 7b) in the matrix. This favorable microstructural features was the key factor that led to the improved thermo-mechanical performance observed in Fig. 6.

Conversely, the colloidal alumina addition spoiled the creep resistance of the alumina–magnesia castable. Although presenting an average pore size slightly higher than the other nanopowders containing castables (Fig. 7b), its poor performance is most likely associated with some drawbacks found during previous processing steps. As mentioned before, due to the interaction between the colloidal alumina suspension and MgO during mixing, a fast gelling process took place and led to large and isolated pores formation. As a consequence, the volume of pores in the matrix was not as reduced as in the nano AM and nano MgO compositions (Fig. 7a) and the creep resistance was directly affected. This result points out that special attention must be taken when adding colloidal alumina suspension as a nano source for spinel castables.

Owing to the excellent results attained, the nano AM castable was selected as the best nano-engineered composition and compared to the reference (REF) and to the M13 A2 one based on two relevant properties: the hot modulus of rupture (HMOR) at 1450 °C and the slag corrosion resistance. For a complete thermo-mechanical and chemical overview, Table 6 presents the results of these experiments and also the maximum

Table 5
Quantitative XRD results of the alumina–magnesia castables fired for 5 h at 1150 °C or 1300 °C [7].

Temperature (°C)	Phase (wt%)	REF	M13 A2	Nano MgO	Nano AM	CA
1150	MgO	3	2	Traces	2	3
	Spinel	9	13	18	16	11
1300	MgO	1	Traces	Traces	Traces	1
	Spinel	18	20	20	18	17

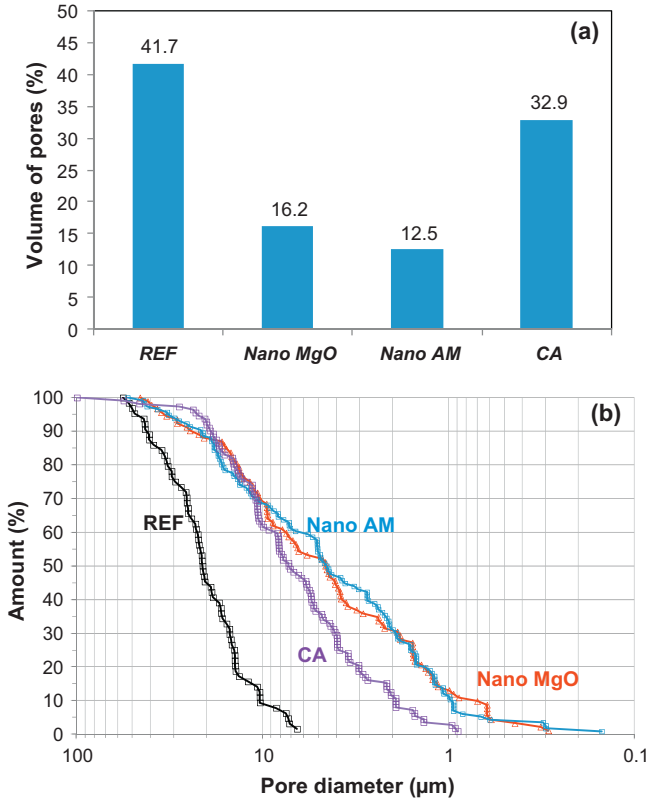

Fig. 7. Volume of pores (a) and pore diameter distribution (b) in the matrix of alumina–magnesia castables (REF, Nano MgO and Nano AM) fired at 1500 °C/5 h.

creep deformation and the overall expansion values of these three selected castables.

Regarding the hot modulus of rupture, the nanopowder addition (nano AM) provided the highest value among the three compositions. However, due to the liquid presence at 1450 °C in such alumina–magnesia castables [13], the attained HMOR for the nano AM sample was still close to the M13 A2 one (Table 4).

A similar situation was observed in the slag resistance experiments. As stated in the previous topic, the microstructural features of *in situ* spinel-forming castables ensure a suitable corrosion resistance when in contact with a steel ladle slag. Thus, the use of finer raw material sources and the consequent benefits pointed out beforehand, had a diminutive effect on this property. In Table 6, it was possible to observe again that, taking the experimental deviations into account, the results of the nano AM and M13 A2 castables were virtually the same.

Table 6
HMOR at 1450 °C, creep deformation (compressive load of 0.2 MPa) at 1450 °C and slag corrosion index after the corrosion experiment for the REF, M13 A2 and Nano AM castables.

	REF	M13 A2	Nano AM
HMOR 1450 °C (MPa)	1.6 ± 0.3	3.7 ± 0.3	4.5 ± 0.4
Creep deformation 1450 °C (%)	1.6	1.0	0.6
Slag corrosion index (%)	8.3 ± 1.1	5.5 ± 1.2	6.0 ± 0.9
Overall expansion (%)	3.6	1.9	1.8

Besides the positive effects on the expansive behavior of alumina–magnesia castables already reported in the literature [5–7], the addition of Al_2O_3 and MgO nanoparticles indeed improved some other relevant properties for castables applied to steel ladles, such as the HMOR and the creep deformation, without decreasing the corrosion resistance. Nevertheless, despite the excellent performance of such nano-engineered castables, the high costs related to nanopowder production should be considered, as micrometric-scaled raw materials may provide very similar results. For all evaluated properties, the use of dead-burnt MgO < 13 μm and a fine alumina mixture (A2) improved the refractory performance, indicating that this is a more interesting formulation approach with an inferior cost.

Although nanotechnology has arisen as an interesting and novel alternative in the materials engineering field, its use in refractory production must be carefully analyzed, as the cost–benefit ratio is still one of the main requirements for the end users.

4. Conclusions

The *in situ* spinel expansion control by adding reactants with reduced grain sizes was confirmed in this work. Among all the evaluated alumina and magnesia sources (micro and nano), the nano AM mixture addition provided the lowest overall expansion. Moreover, it also ensured the best results regarding the material's thermo-mechanical (HMOR and creep) and thermo-chemical (corrosion resistance) performance, which pointed out nanotechnology as an apparent novel and efficient option to improve the spinel refractory castables' working life.

However, the overall expansion and the performance at high temperatures of the castable designed by micrometric-sized Al_2O_3 and MgO particles (M13 A2) were almost as suitable as the nano AM composition. Therefore, considering that the cost–benefit ratio is still one of the main requirements for the refractories users, the development of nanoengineered castables in this system is actually not so effective, and it may only be considered a feasible tool when the high cost associated with the raw materials production is overcome or the performance would be much better.

Acknowledgments

The authors are grateful to FIRE (Federation for International Refractories Research and Education) and the Brazilian research funding CNPq for supporting this work. The authors would also like to thank Dr. Ana P. Luz for helping with the corrosion rate measurements and G.G. Morbioli for the castable's processing steps.

References

[1] C. Wagner, The mechanism of formation of ionic compounds of higher order (double salts, spinel, silicates), Zeitschrift fur Physikalische Chemie B34 (1936) 209–316.
[2] R.E. Carter, Mechanism of solid-state reaction between magnesium oxide and aluminum oxide and between magnesium oxide and ferric oxide, Journal of the American Ceramic Society 44 (3) (1961) 116–120.

[3] Z. Nakagawa, Expansion behavior of powder compacts during spinel formation, Mass and Charge Transport in Ceramics (1996) 283–294.
[4] E.Y. Sako, M.A.L. Braulio, E. Zinngrebe, S.R. van der Laan, V.C. Pandolfelli, Fundamentals and applications on in situ spinel formation mechanisms in Al_2O_3–MgO refractory castables, Ceramics International (2011), doi:10.1016/j.ceramint.2011.10.074.
[5] M.A.L. Braulio, J.F. Castro, C. Pagliosa, L.R.M. Bittencourt, V.C. Pandolfelli, From macro to nanomagnesia: designing the *in situ* spinel formation, Journal of the American Ceramic Society 91 (9) (2008) 3090–3093.
[6] M.A.L. Braulio, M.F.L. Piva, G.F.L. Silva, V.C. Pandolfelli, In situ spinel expansion designed by colloidal alumina addition, Journal of American Ceramic Society 92 (2) (2009) 559–562.
[7] M.A.L. Braulio, G.G. Morbioli, L.R.M. Bittencourt, V.C. Pandolfelli, Novel features of nanoscaled particles addition to alumina–magnesia refractory castables, Journal of American Ceramic Society 93 (9) (2010) 2606–2610.
[8] T.R. Lipinski, C. Tontrup, The use of nano-scaled alumina in alumina-based refractory materials, in: Proc. UNITECR 2007, Dresden, Germany, (2007), pp. 391–393.
[9] E.Y. Sako, M.A.L. Braulio, D.H. Milanez, P.O. Brant, V.C. Pandolfelli, Microsilica role in the CA_6 formation in cement-bonded spinel refractory castables, Journal of Materials Processing Technology 209 (2009) 5552–5557.
[10] E.Y. Sako, M.A.L. Braulio, V.C. Pandolfelli, The corrosion and microstructure relationship for cement-bonded spinel refractory castables, Ceramics International (2011), doi:10.1016/j.ceramint.2011.10.061.
[11] M.A.L. Braulio, A.P. Luz, A.G. Tomba Martinez, C. Liebske, V.C. Pandolfelli, Basic slag attack of spinel-containing refractory castables, Ceramics International 37 (6) (2011) 1935–1945.
[12] B.A. Vázquez, A. Caballero, P. Pena, Quaternary system Al_2O_3–CaO–MgO–SiO_2. II. Study of the crystallisation volume of $MgAl_2O_4$, Journal of American Ceramic Society 88 (7) (2005) 1949–1957.
[13] E.Y. Sako, M.A.L. Braulio, P.O. Brant, V.C. Pandolfelli, The impact of pre-formed and in situ spinel formation on the physical properties of cement-bonded high alumina refractory castables, Ceramics International 36 (2010) 2079–2085.
[14] A.D. Smigelskas, E.O. Kirkendall, Zinc diffusion in alpha brass, Transactions of the AIME 171 (1947) 130–142.
[15] H.J. Fan, M. Knez, R. Scholz, K. Nielsch, E. Pippel, D. Hesse, M. Zacharias, U.G. Sele, Monocrystalline spinel nanotube fabrication based on the Kirkendall effect, Nature Materials 5 (2006) 627–631.
[16] H. Sarpoolaky, K.G. Ahari, W.E. Lee, Influence of in situ phase formation on microstructural evolution and properties of castables refractories, Ceramics International 28 (5) (2002) 487–493.